Available online at www.sciencedirect.com

ScienceDirect

Energy Procedia 142 (2017) 1306–1311

Energy Procedia

www.elsevier.com/locate/procedia

9th International Conference on Applied Energy, ICAE2017, 21-24 August 2017, Cardiff, UK

# Numerical Study of the Effects of $CO_2$ Addition in Single Coal Particle Gasification

Tata Sutardi, Manosh C. Paul*, Nader Karimi and Paul L. Younger

*Systems, Power & Energy Research Division, School of Engineering, University of Glasgow Glasgow G12 8QQ, UK*

**Abstract**

Gasification appears to be the way of processing and utilizing coal cleanly. However, currently the main issue of coal utilization is $CO_2$ production that adversely impacts the environmental sustainability of this process. Some efforts have been made to control and reduce the $CO_2$ emission in the atmosphere, such as using CCS (Carbon Captured and Storage) or CCU (Carbon Captured and Utilization). As a part of those efforts, this work investigates the effect of utilizing $CO_2$ in the gasification process. Towards this aim, numerical simulations of single coal particle gasification are conducted. The benefits of adding $CO_2$ to the gasification process compared to that of air are examined thoroughly. It is found that $H_2$, CO and $CH_4$ productions are increased with $CO_2$ addition thus indicating an improvement in syngas generation from the coal gasification.

© 2017 The Authors. Published by Elsevier Ltd.
Peer-review under responsibility of the scientific committee of the 9th International Conference on Applied Energy.

*Keywords:* Gasification; $CO_2$ utilization; Single coal particle model; Numerical simulation; syngas production

**Nomenclature**

| Roman Symbol | | | |
|---|---|---|---|
| $h_s$ | Heat source (W/m$^2$ K) | $p$ | Pressure (Pa) |
| $A$ | Pre- exponential factor (unit vary) | $m_i$ | Mass fraction |
| $E_a$ | Activation Energy (J/kmol) | $C_{\varepsilon 1}$; $C_{\varepsilon 2}$ | Model constant |
| $R$ | Gas universal constant (J/kmol K) | $t$ | Time (s) |
| $k_i$ | Reaction rate coefficient for | $x$ | Distance/displacement (m) |
| | | $u$ | Velocity (m/s) |

* Corresponding author. Tel.: +44 (0) 141 3308466
*E-mail address:* Manosh.Paul@glasgow.ac.uk

1876-6102 © 2017 The Authors. Published by Elsevier Ltd.
Peer-review under responsibility of the scientific committee of the 9th International Conference on Applied Energy.
10.1016/j.egypro.2017.12.506

| | | | |
|---|---|---|---|
| $p_{ij}$ | Rate exponent of reacting species | $\Gamma_i$ | Fick diffusion coefficients |
| $h$ | Enthalpy (kJ/kg) | $\rho g_i$ | Gravitational body force |
| $J_i$ | The flux of species $i$ | $\mu$ | Viscosity (kg/m.s) |
| $T$ | Temperature (K) | $\sigma$ | Turbulent Prandtl number |
| $YY$ | Mass stoichiometric coefficient | $\delta$ | Kronecker delta |
| Greek Symbol | | Subscript | |
| $\beta$ | Temperature exponent | $i, j$ | Species or phase |
| $\tau_{ij}$ | Stress tensor | $k$ | Turbulent kinetic energy ($m^2/s^2$) |
| $\rho$ | Density ($kg/m^3$) | $\varepsilon$ | Turbulent dissipation rate ($m^2/s^3$) |

## 1. Introduction

According to the International Energy Outlook (IEO) 2016 [1], the world energy related $CO_2$ emissions increase at an average annual rate of 1% from 2012 to 2040. Coal, being the most carbon-intensive fossil fuel, became the leading source of world energy-related $CO_2$ emissions in 2006, and it remains to be the leading source of energy through 2040 [1]. However, although coal accounted for 39% of total $CO_2$ emissions in 1990 and 43% in 2012, its share is projected to decline to 38% in 2040 [1]. This declining is predicted because of more utilization of clean coal technologies in future. Coal gasification is one of those technology options.

Gasification becomes attractive since this technology allows conversion of coal to chemical stocks or fuel in a more environmentally friendly fashion in comparison to combustion. One of the reduction potency comes by utilizing $CO_2$ into the gasification process. In order to explore this potency, a single coal particle gasification model has been developed to study the effects of $CO_2$ addition as the gasification agent of a single coal particle. The focus of this investigation is on the comparison of syngas products. The outcomes of the current study are deemed applicable to further advancements of coal gasification technology.

## 2. Simulation Model Development

Simulation model was initially developed based on the experimental study of coal combustion presented in Ref. [2]. This was then extended further by adding suitable chemical reactions to the model for investigating coal particle gasification. Simulated results of the coal particle combustion were validated with the experimental results [3]. Subsequently, a single coal particle into the drop tube furnace (DTF) was injected for gasification process simulation and investigation. The schematic view of the physical model and the computational domain of the reactor is illustrated in Fig. 1[2].

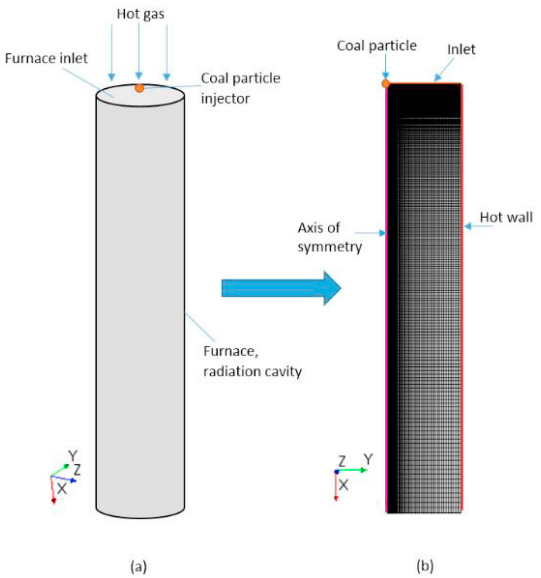


Fig. 1. The reactor illustration (a) Schematics of the reactor (b) Axisymmetric computational domain.

The DTF is represented as a cylindrical shape geometry as illustrated in Fig. 1(a), with the inlet diameter of 7 cm,

and the hot wall reactor length of 25 cm from the inlet. The coal particle injection starts from the centre of the inlet. The axisymmetric model with grid distribution used for the simulation can be seen in Fig. 1(b). The validation process of the current simulations has been discussed in the previous paper [3] and will not be repeated here.

The main physicochemical processes occurring during coal gasification are drying, devolatilization/pyrolysis, combustion and gasification. The pertinent chemical reactions are presented in Table 1 below.

Table 1. Reactions of the gasification process

| Mechanisms | Reaction | Kinetic parameter | | | Ref |
|---|---|---|---|---|---|
| | | $A$ (vary) | $E_a$ (j/kmol) | $\beta$ | |
| Rawcoal → YY Coal volatile + (1 –YY) Char | R1 | 3.12 E+05 | 7.4 E+07 | 0 | [4] |
| $C + O_2 \rightarrow CO_2$ | R2 | 2 E+1 | 7.9 E+07 | 0 | [3] |
| $C + 0.5O_2 \rightarrow CO$ | R3 | 1 E+3 | 1.33 E+08 | 1 | [3] |
| $C + CO_2 \rightarrow 2CO$ | R4 | 4.4 | 1.62 E+08 | 1 | [5] |
| $C + H_2O \rightarrow CO + H_2$ | R5 | 1.33 | 1.47 E+08 | 1 | [5] |
| $C + 2H_2 \rightarrow CH_4$ | R6 | 1 E+3 | 1.131 E+08 | 0 | [6] |
| Coal Volatile + $O_2 \rightarrow CO_2 + H_2O + N_2$ | R7 | 2.119 | 2.027 E+08 | 0 | [4] |
| $CO + 0.5O_2 \rightarrow CO_2$ | R8 | 1.3 E+11 | 1.26 E+08 | 0 | [7] |
| $H_2 + 0.5O_2 \rightarrow H_2O$ | R9 | 1.5 E+13 | 2.85 E+08 | 0 | [6] |
| $CO + H_2O \rightarrow CO2 + H_2$ | R10 | 4.2 E+07 | 1.383 E+08 | 0 | [6] |
| $CH_4 + H_2O \rightarrow CO + 3H_2$ | R11 | 4.4 E+11 | 1.68 E+08 | 0 | [6] |
| $CH_4 + 0.5O_2 \rightarrow CO + 2H_2$ | R12 | 3 E+08 | 1.26 E+08 | -1 | [6] |
| $CH_4 + CO_2 \rightarrow 2CO + 2H_2$ | R13 | 4.6 E+11 | 3.124 E+08 | 0.3 | [8] |

As seen in Table 1, the reactions mechanism of coal gasification consists of thirteen chemical reactions [9]. The R2 to R6 are heterogeneous reactions (gas-solid), while R7 to R13 are homogeneous reactions (gas-gas).

### 2.1 Governing equations

The governing equations used for fluid interactions in this simulation are the equations of continuity of mass, transport of momentum, transport of chemical species and conservation of energy [10].

The law of mass conservation results in the mass continuity equation as shown below:

$$\frac{\partial \rho}{\partial t} + \frac{\partial (\rho u_i)}{\partial x_i} = 0. \tag{1}$$

The equation for the transport of momentum is represented by [10]:

$$\frac{\partial (\rho u_i)}{\partial t} + \frac{\partial (\rho u_i u_j)}{\partial x_j} = \frac{\partial p}{\partial x_i} + \frac{\partial \tau_{ij}}{\partial x_j} + \rho g_i, \tag{2}$$

where $p$ is the static pressure, $\tau_{ij}$ is the stress tensor, $\rho g_i$ is the gravitational body force. The stress tensor $\tau_{ij}$ for a Newtonian fluid is defined by [10]:

$$\tau_{ij} = \left[\mu\left(\frac{\partial u_i}{\partial x_j} + \frac{\partial u_j}{\partial x_i}\right)\right] - \frac{2}{3}\mu \frac{\partial u_l}{\partial x_l}\delta_{ij} \tag{3}$$

The concentration of each species can be expressed in terms of the mass fraction $m_i(x,t)$, or the concentration of species $C_i = m_i \rho$, which is defined as the mass of species per unit volume.

The conservation law of chemical species $i$ is represented as

$$\frac{\partial}{\partial t}(\rho m_i) + \nabla \cdot (\rho m_i V)) = R_i + \Gamma_i \nabla^2 m_i, \tag{4}$$

where $R_i$ is the account for the production or consumption of the species by chemical reactions, and $\Gamma_i$ is the Ficks diffusion coefficients.

The energy equation in this simulation may be written as [10]:

$$\frac{\partial (\rho h)}{\partial t} + \frac{\partial (\rho u_i h)}{\partial x_i} = \frac{\partial}{\partial x_i}\lambda \frac{\partial T}{\partial x_i} - \frac{\partial \sum_j h_j J_j}{\partial x_i} + \frac{Dp}{Dt} + (\tau_{ik})\frac{\partial u_i}{\partial x_k} + h_s \tag{5}$$

In this equation $h$ is the enthalpy and $h_s$ includes heat of chemical reaction, any inter-phase exchange of heat, and any other user defined volumetric heat sources.

In this simulation, the fluid in the reaction is treated as an ideal gas. The ideal gas equation is expressed as

$$\frac{p}{\rho} = RT \tag{6}$$

$R$ is universal gas constant.

In this simulation, RANS (Reynolds-Averaged Navier-Stokes) approach was used for handling the effects of turbulence. These equations describe the behaviour of the time-averaged flow quantities instead of the exact instantaneous values. In this approach, RANS equations arise when the Reynolds decomposition is implemented into the Navier-Stokes equations.

The RANS equation is represented as,

$$\rho\frac{\partial(\bar{u}_i)}{\partial t} + \rho\frac{\partial\left((\bar{u}_i\bar{u}_j)\right)}{\partial x_j} = -\frac{\partial(\bar{p})}{\partial x_i} + \mu\nabla^2\bar{u}_\iota - \frac{\partial\tau_{ij}}{\partial x_j} \tag{7}$$

The equations above are not closed because the component Reynold stress tensor $\tau_{ij}$, is unknown and cannot be expressed as a function of $(\bar{u})$ and $(\bar{p})$. In order to solve this equation a turbulence model is needed and this simulation uses the realizable $k-\varepsilon$ model. The $k$ model is transport equation for turbulent kinetic energy, and may be represented as

$$\rho\frac{\partial k}{\partial t} + \rho(\bar{u}_j)\frac{\partial k}{\partial x_j} = 2\mu\bar{S}_{ij}\frac{\partial(\bar{u}_i)}{\partial x_j} - \rho\varepsilon + \frac{\partial}{\partial x_j}\left[\left(\mu + \frac{\mu_t}{\sigma_k}\right)\frac{\partial k}{\partial x_j}\right] \tag{8}$$

while, the $\varepsilon$ model is the transport equation for viscous dissipation (the rate at which the kinetic energy of small scale fluctuation is converted into heat by viscous friction), and it represented as,

$$\rho\frac{\partial\varepsilon}{\partial t} + \rho\left(\bar{u}_j\right)\frac{\partial\varepsilon}{\partial x_j} = C_{\varepsilon1}P_k\frac{\varepsilon}{k} - C_{\varepsilon2}\rho\frac{\varepsilon^2}{k} + \frac{\partial}{\partial x_j}\left[\left(\mu + \frac{\mu_t}{\sigma_\varepsilon}\right)\frac{\partial\varepsilon}{\partial x_j}\right] \tag{9}$$

In this simulation the constant used for the equation above are: $C_{\varepsilon1} = 1.44$ ; $C_{\varepsilon2} = 1.9$ ; $\sigma_k = 1$ ; $\sigma_\varepsilon = 1.2$ .

The commercial software Star CCM+ was used to run the simulations.

### 2.3 Boundary conditions and coal properties

The initial boundary condition is taken from the experimental study [2]. The inlet was set as velocity inlet, with initial temperature of hot air being 1200 K and at the same time the reactor wall was set as hot wall with temperature of 1400 K. In order to minimize the effect of air flow velocity on the coal particle, the simulation is conducted under a quiescent gas condition in the reactor and it is set by turning off the hot air flows a few seconds prior to the particle injection. The coal particle diameter is $75\mu m$ as this size is commonly used in pulverize coal power plants and modelled as a spherical shape. The chemical properties of coal particle is taken from proximate and ultimate analysis, as shown in Table 2 [2].

Table 2. Chemical composition of the coal PSOC 1451

| Proximate Analysis as receives | value | Ultimate Analysis (dry basis) | value |
|---|---|---|---|
| Moisture ( % ) | 2.5 | Carbon ( % ) | 71.9 |
| Volatile matter ( % ) | 33.6 | Hydrogen ( % ) | 4.9 |
| Fixed Carbon ( % ) | 50.6 | Oxygen (%) (by diff.) | 6.9 |
| Ash ( % ) | 13.3 | Nitrogen (%) | 1.4 |
| | | Heating value dry fuel (MJ/kg) | 31.5 |

Since the current focus is on the gasification reactions as stated in the Table 1, only element C, H, O, and N are used from the ultimate Dry-Ash Free (DAF) to define the raw coal. Based on the proximate and ultimate correlation, the coal volatile composition for PSOC 1451 is defined as $CH_{2.7}O_{0.248}N_{0.058}$ or the *YY* value 0.29 as stated in the reaction balance equation R1[11].

## 3. Results

Since the oxidation stage of this model has been validate [3], this section only explores the potency of $CO_2$ utilization on the gasification process. Gasification process in this model has been developed by including all the reactions as stated in Table 1. The current study compares the results of gasification of a single coal particle in air and that in a gas atmosphere consisting of 20% $CO_2$, 20% $O_2$ and 60% $N_2$. The simulation results for the comparison of particle temperature and char mole fraction can be seen in Fig. 2a, and Fig. 2b shows a comparison between the

productions of CO and $H_2$ in the two investigated gas atmospheres.

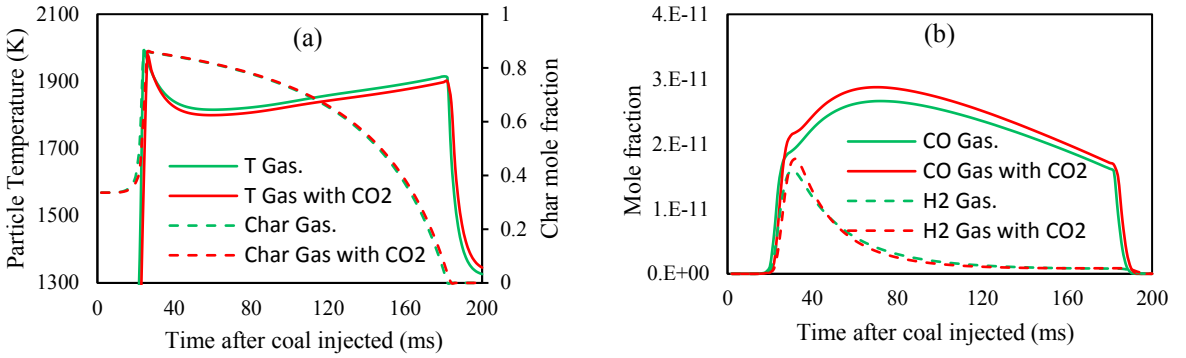


Fig. 2. The gasification result of air and $CO_2$ agent for (a). Temperature (b). CO and $H_2$ mole fraction.

Fig. 2a shows that during the gasification process, the maximum particle temperature with only air is slightly higher than that with addition of $CO_2$. Both conditions occur on the coal volatile reaction and char reaction as seen as on the peaks of the temperature profiles in Fig. 2. The same figure indicates that the char mass fraction trajectory in $CO_2$ enriched atmosphere lasts slightly longer than that in pure air. Adding $CO_2$ reduces the char reaction rate in the coal particle, resulting in increased production of CO, as illustrated in Fig. 2b.

Other advantage comes from hydrogen production. Figure 2 indicates that the maximum $H_2$ production under the condition of $CO_2$ addition is higher than that in pure air as the gasification agent. Other comparison for this investigation is done on the basis of $CH_4$ production. Fig. 3 depicts the molar generation of this gas under the two investigated gas atmospheres. It can be seen that in the case of $CO_2$ addition, the maximum $CH_4$ generation is higher than that under pure air. However, at the same time, Fig. 3 shows that the addition of $CO_2$ has a negligible effect on $H_2O$ production.

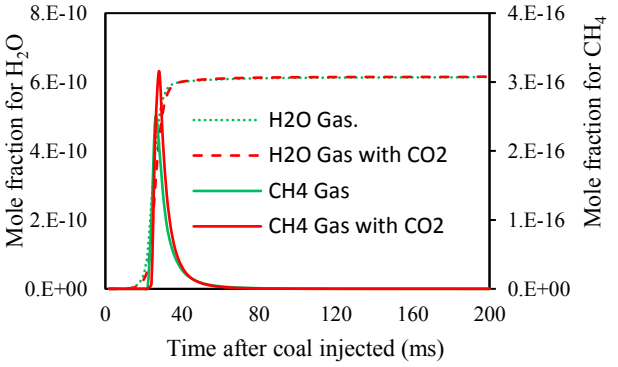


Fig. 3. $CH_4$ and $H_2O$ comparison for single coal particle gasification

## 4. Conclusion

A single particle simulation model has been developed and the effects of $CO_2$ addition on the gasification process of a single coal particle was investigated. The numerical simulations showed that the addition of $CO_2$ has potency for increasing syngas components such as CO, $H_2$ and $CH_4$. The presented results were based on the comparisons between the air only and air with $CO_2$ addition applied as the gasification agent of a single coal particle. The outcomes have indicated the favourable effects of $CO_2$ addition to the gasification process. Thus, this study can potentially have important benefits for the development of clean coal technology with CCU application.

**Acknowledgements**

The first author acknowledges the scholarship support from the Ministry of Research and Higher Education (KEMENRISTEKDIKTI) and the Agency for the Assessment and Application of technology (BPPT) Republic of Indonesia through the RISET-Pro (Research & Innovation Science & Technology) Program, and also the research support from the University of Glasgow.

**References**

[1] DOE/EIA, *International Energy Outlook 2016.* US Energy Information Administration, 2016. **0484**.
[2] Levendis, Y.A.J., Kulbhushan. Khatami, Reza. Sarofim, Adel F., *Combustion behavior in air of single particles from three different coal ranks and from sugarcane bagasse.* Combustion and Flame, 2011. **158**(3): p. 452-465.
[3] T. Sutardi, M.C.P., N. Karimi and Paul L. Younger, *Identifying Kinetic Parameters for Char Combustion of a Single Coal Particle.* Eurpean Combustion Meeting, 2017. **ISBN 978-953-59504-0-0**(2017): p. 247.
[4] *Fluent 6.3 user's guide.* Fluent Inc., 2005.
**[5]** AM., M., *The rate of reduction of carbon dioxide by graphite.* Am Chem Soc J, 1934. **56:70–6.**
[6] Zogala, A., *CRITICAL ANALYSIS OF UNDERGROUND COAL GASIFICATION MODELS. PART II: KINETIC AND COMPUTATIONAL FLUID DYNAMICS MODELS.* Journal of Sustainable Mining, 2014.
[7] Alganash, B., M.C. Paul, and I.A. Watson, *Numerical investigation of the heterogeneous combustion processes of solid fuels.* Fuel, 2015. **141**: p. 236-249.
[8] Sun, Z., Wu, J., Wang, Y., Zhang, D. , *A kinetic study of CO2 gasification of a Chinese coal char during combined coal gasification and CH4 reforming.* Journal of Fuel Chemistry and Technology, 2009.
[9] Żogała, A. and T. Janoszek, *CFD simulations of influence of steam in gasification agent on parameters of UCG process.* Journal of Sustainable Mining, 2015. **14**(1): p. 2-11.
[10] Zikanov, O., *Essential Computational Fluid Dynamics.* 2012.
[11] Piyush Thakre, R.R., *Setting up Coal Combustion in STARCCM+5.04.* 2010.